ASME Journal of Biomechanical Engineering
Online journal at:
https://asmedigitalcollection.asme.org/biomechanical

Optimal Powered Ankle–Foot Prosthesis Torque Profiles to Improve Walking Performance for Individuals With a Unilateral Transtibial Amputation

Eric H. Hu
Walker Department of Mechanical Engineering,
The University of Texas at Austin,
204 East Dean Keeton Street,
Austin, TX 78712-1591
e-mail: eh32733@eid.utexas.edu

Glenn K. Klute
Department of Veterans Affairs,
Puget Sound Health Care System,
1660 South Columbian Way, MS-151,
Seattle, WA 98118;
Department of Mechanical Engineering,
University of Washington,
3900 East Stevens Way NE,
Seattle, WA 98195
e-mail: gklute@uw.edu

Richard R. Neptune[1]
Mem. ASME
Walker Department of Mechanical Engineering,
The University of Texas at Austin,
204 East Dean Keeton Street,
Austin, TX 78712-1591
e-mail: rneptune@mail.utexas.edu

Prosthetic ankle–foot devices provide valuable assistance for individuals with a unilateral transtibial amputation (TTA) to effectively engage in daily living activities, although users often experience diminished walking performance such as increased metabolic cost, knee joint loading, and dynamic balance asymmetry due to the lack of torque control from commonly prescribed passive devices. Consequently, active powered prosthetic devices have been developed; however, it is unclear how to optimally tune them. The purpose of this study was to identify the optimal ankle torque profile of a powered ankle–foot prosthesis that improves walking performance for individuals with TTA. Specifically, we used a musculoskeletal simulation-based optimization framework to optimize a powered prosthesis torque profile while emulating group averaged kinematics and ground reaction forces (GRFs). We compared the metabolic cost, knee joint loading, sagittal plane dynamic balance symmetry, and torque profiles across the following simulated conditions: a passive prosthesis tracking individuals with TTA walking data, a powered prosthesis tracking able-bodied walking data, and a powered prosthesis that separately minimized metabolic cost, knee joint loading, and dynamic balance asymmetry. Distinct torque profiles emerged for each measure, but there was no clear trend in the positive prosthetic work performed, which suggests increased prosthetic work alone is insufficient to improve walking performance. Further analysis showed the prosthetic torque must be properly timed over the gait cycle to improve each measure. This study provides a framework for future work developing customized controllers for powered prostheses to improve various aspects of walking performance for individuals with TTA. [DOI: 10.1115/1.4071411]

Keywords: biomechanics, below-knee amputee, gait, prosthesis, modeling, optimization

Introduction

Prosthetic ankle–foot devices are indispensable components that individuals with a unilateral transtibial amputation (TTA) rely on to effectively engage in activities of daily living. Although such devices can help improve mobility, the use of commonly prescribed passive ankle–foot prostheses can lead to asymmetric walking patterns, compensatory mechanisms, and the development of secondary injuries [1]. For example, previous studies have shown that individuals who use passive ankle–foot prostheses experience increased metabolic cost [2,3] and joint loading that can increase the risk of developing osteoarthritis on the intact limb knee [4] as well as soft tissue injury at the socket-residual limb interface [5]. TTAs have also demonstrated a higher prevalence of falling, which may be indicative of poor dynamic balance [6,7]. Previous research analyzing dynamic balance during walking using the range of whole-body angular momentum found asymmetric values between steps in the sagittal plane, which was correlated with reduced residual limb propulsion from their passive prosthetic ankle–foot devices [7].

To address these walking deficits, powered ankle–foot prostheses have been developed to deliver more biologically representative ankle power throughout the gait cycle. Studies have shown that powered prostheses can reduce the metabolic cost of walking relative to passive prostheses to levels comparable to able-bodied individuals [8,9]. In addition, powered prostheses have demonstrated a reduction in peak resultant ground reaction forces (GRFs)

[1]Corresponding author.
Manuscript received September 3, 2025; final manuscript received March 12, 2026; published online April 8, 2026. Assoc. Editor: Matty J. Major.

and external knee adduction moments, which are common surrogate measures of knee joint loading [10]. Others have found that powered prostheses can provide better dynamic balance in the sagittal plane compared to passive prostheses at certain walking speeds but were not able to produce symmetrical ranges of whole-body angular momentum between steps [11]. These studies used commercial powered prostheses of which only the ankle stiffness and power delivery were adjusted. However, it is unclear if there is an optimal torque profile that can reduce these walking deficits and produce more able-bodied walking mechanics.

Forward dynamics simulations using detailed musculoskeletal models can identify causal relationships between various control inputs and the resulting gait performance. For example, previous research has used simulations to identify the optimal muscle excitation patterns required to predict an accurate estimate of able-bodied and pathological gait [12,13]. Specifically for a powered ankle–foot prosthesis, a control mechanism was identified that reduced the metabolic cost of walking to values below that of able-bodied individuals; however, the resulting gaits were highly asymmetric and deviated from experimental able-bodied gait mechanics [14]. Thus, further research is needed to assess whether there exist optimal torque profiles that improve various biomechanical measures of TTA gait while producing able-bodied walking patterns.

The purpose of this study was to identify the optimal ankle torque profile of a powered prosthesis that improves steady-state walking performance for individuals with TTA using a musculoskeletal simulation-based optimization framework. Specifically, we sought to identify the torque profile that improves metabolic cost, joint loading, and dynamic balance symmetry while producing able-bodied gait mechanics. We expected that a distinct optimal ankle torque profile exists to improve each aspect of walking performance. The outcomes of the work provide the basis for future powered prosthesis control designs aimed at improving rehabilitation outcomes for those with TTA.

Methods

Experimental Data. Lower-limb joint kinematics and GRFs of nine participants with TTAs and nine healthy able-bodied participants were previously collected from separate studies walking at their self-selected walking speed (TTA: 1.26±0.2 m/s, able-bodied: 1.30±0.2 m/s). For each dataset, joint kinematics, GRFs (normalized by body weight (BW)), and whole-body angular momentum (normalized by body mass, height, and walking speed) were normalized to a single stride from heel strike to heel strike and averaged across all trials. These datasets and walking speed for each subject group were then group averaged, and the means and standard deviations were used in the objective functions for the various optimizations. For more details regarding the data collection and processing, please see Refs. [15] and [16].

Musculoskeletal Model. A 2D musculoskeletal model was modified from the H0918 SCONE model from a previous study [17] to represent a unilateral right transtibial amputee (Fig. 1). All joints were constrained with a passive torque using a coordinate limit force to ensure a normal range of motion [18]. A compliant foot–ground contact model [19] was used with contact spheres added to the toe and heel of each foot with a radius of 3 cm, a stiffness coefficient of 2,000,000 N/m, a dissipation constant of 1.0 s/m, a static friction coefficient of 0.9 (unitless), a dynamic friction coefficient of 0.6 (unitless), a viscous friction coefficient of 0.6 (unitless), and a transition velocity of 0.15 m/s.

The model was actuated by 20 Hill-type musculotendon actuators (Table 1) using Millard-type muscle properties. The muscle excitations were represented with a combination of feedforward and feedback control. For the feedforward control, one or more rise–fall functions [20] with four optimizable parameters, including start time, rise time, fall time, and peak amplitude, were used for each muscle group with the timing loosely constrained based on

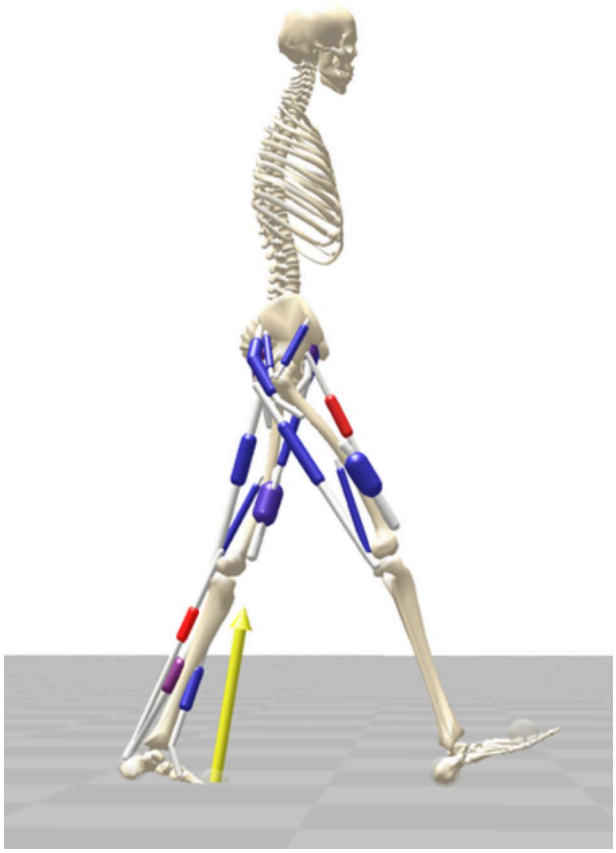

Fig. 1 The musculoskeletal model of an individual with a transtibial amputation. The model had a mass of 72.2 kg and height of 1.8 meters with 20 Hill-type muscle group actuators and a coordinate actuator on the right ankle joint to represent the ankle–foot prosthesis.

electromyography recordings in the literature [21]. For the feedback control, a neuromuscular reflex controller was used to optimize the muscle length, velocity, force, and spindle force feedback gains according to specific phases of the gait cycle [22] determined by the sagittal foot position and normalized GRF of each leg.

To model the prosthetic ankle, the soleus, gastrocnemius, and the tibialis anterior were removed from the right leg, and a coordinate actuator was added to the right ankle joint to provide a torque that replicates the elastic properties of a passive prosthetic ankle–foot

Table 1 Muscle group and ankle actuators within the musculoskeletal model and their corresponding abbreviations

Muscle group actuator	Muscle abbreviation
Hamstring (biarticular)	HAMS
Bicep femoris short head	BFSH
Gluteus maximus	GMAX
Iliopsoas	ILPS
Rectus femoris	RF
Vasti	VAS
Gluteus medius (anterior + posterior)	GMED
Gastrocnemius[a] (medial + lateral)	GAS
Soleus[a]	SOL
Tibialis anterior[a]	TA
Ankle motor[b]	Prosthesis

[a]Indicates muscle actuator is only present in the intact limb only.
[b]Indicates muscle actuator is only present in the residual limb only.

device and an ideal motor of a powered prosthetic ankle. The mass and inertial properties of the right tibia were modified by combining the properties of the transected tibia and pylon socket, and the right foot was adjusted by combining the properties of the foot components based on LaPrè et al. [23]. The torque profile of the coordinate actuator for both the passive and powered prosthetic ankles was a transient function composed of a set of 11 rise–fall patterns and a proportional derivative control mechanism with parameters optimized throughout the gait cycle.

Optimizations

Overall Framework. All optimizations were run using SCONE (v. 2.4.1), which is an open-source software for generating forward dynamics simulations using optimization with high-level objectives [24]. The software uses Covariance Matrix Adaptation-Evolution Strategy to optimize the model's actuator parameters [25]. For the present study, three optimizations ran in parallel with each having a different random seed, giving a broader search space to optimize a total of 209 parameters for each simulation. The best solution from the set of parallel optimizations was selected, and the parameters were then seeded for another set of parallel optimizations. This process was repeated until there was no further change in the cost function. The final converged results were then imported to MATLAB (Mathworks, Natick, MA) for analysis. All optimizations were run on a desktop computer with a 4 GHz AMD Ryzen Threadripper Pro processor, with each optimization typically converging within ten hours.

Simulation of Transtibial Amputee Walking Mechanics With a Passive Prosthetic Ankle. To provide a benchmark comparison, the walking pattern of individuals with TTA wearing a passive prosthetic ankle (PASS) was simulated. The initial state of the model was assigned to be the joint position and velocities at time zero of the TTA experimental data so that the simulations began with a realistic configuration and the overall computational time was reduced. To model the passive prosthetic ankle, the stiffness and damping parameters of coordinate limit force on the right ankle joint were manually adjusted so that the prosthesis provided adequate force during stance but also constrained the ankle angle to within ± 0.2 deg of the experimental ankle angle during the swing phase. For the tracking optimization, the cost function (Eq. (1)) was set to minimize a weighted sum of (1) the squared differences of the simulated and experimental hip, knee, and ankle kinematics and vertical and anterior–posterior GRFs normalized by the respective experimental standard deviation squared for both limbs [26], (2) the metabolic cost based on the model in Ref. [27] that estimates total metabolic cost based on heat released and the work performed by the muscles [28], (3) the absolute difference of the simulated and experimental average walking speed, and (4) a pelvis tilt constraint

$$J = \sum_{j=1}^{m}\sum_{i=1}^{n} w_j * \frac{\left(Y_{ij} - \hat{Y}_{ij}\right)^2}{\mathrm{SD}_{ij}^2} + \sum_{j=1}^{m} w_{\mathrm{period}} * \left(\hat{Y}_{\mathrm{end},j} - \hat{Y}_{1,j}\right) + w_{\mathrm{met}} * \mathrm{Met} + w_v * \mathrm{abs}\left(v_{\mathrm{sim}} - v_{\mathrm{exp}}\right) + w_p * \mathrm{Pel}_{\mathrm{tilt}} \quad (1)$$

where w_j is the weighting factor for each of the kinematics and GRF terms, Y_{ij} is the averaged experimental measurement of the jth term at time-step i, $\hat{Y}_{ij}$ is the simulated jth term at time-step i, SD_{ij} is the averaged standard deviation of the jth term at time-step i, n is the number of time-steps, m is the number of kinematics and GRF tracking terms, w_{period} is the weighting factor of the periodicity constraint for each kinematic and GRF term between the first ($\hat{Y}_{1,j}$) and last ($\hat{Y}_{\mathrm{end},j}$) time points of the gait cycle, w_{met} is the weighting factor of the metabolic cost (Met) calculated as the average muscle energy expenditure normalized by distance traveled (i.e., cost of transport) and body mass at time-step i, w_v is the weighting factor for the absolute difference between the simulated center of mass average forward velocity (v_{sim}) and the experimental average walking speed (v_{exp}), and w_p is the weighting factor for the pelvis tilt constraint ($\mathrm{Pel}_{\mathrm{tilt}}$). To achieve the lowest possible cost function value, w_j was iteratively adjusted while w_{met} was set to one to ensure a reasonable metabolic cost without excessively influencing the resulting kinematics and GRFs, w_v was set to 10,000 to ensure the model walked at the desired experimental speed, and w_p was set to five to maintain an upright walking posture without also excessively influencing the other cost function measures.

Simulation of Able-Bodied Walking Mechanics With a Powered Prosthetic Ankle. The walking pattern of able-bodied individuals was simulated with the TTA model and a powered prosthetic ankle (POW) using a similar framework. The initial state of the model was assigned to be the joint position and velocities at time zero of the able-bodied experimental data, and the same cost function equation (Eq. (1)) was used to track able-bodied experimental data. The weighting factors for the kinematics and GRF tracking terms were iteratively adjusted to achieve the lowest possible cost function value while maintaining the weighting factors for the other cost function measures identical to those used in the TTA tracking cost function.

Simulation of Able-Bodied Walking Mechanics With Additional Criteria. The control parameters of the best tracking result for the powered prosthetic ankle were then seeded into subsequent optimizations to improve different measures of walking performance. For each additional criterion, the initial weighted contribution was set to be 20% of the total cost function value from the best able-bodied walking mechanics result, ensuring that the additional term would influence but not dominate the optimized result. The weighting factor would then be scaled based on the unweighted value of each additional criterion so that the initial weighted contribution matched the target proportion. When minimizing metabolic cost (MC), Eq. (1) was used with the same weighting factors as in the POW condition with exception of the metabolic cost weighting factor being assigned the new scaled weighting factor. When minimizing joint loading, the joint contact force terms for both the intact limb (Eq. (2)) and residual limb (Eq. (3)) were added

$$J_{\mathrm{IJL}} = w_{\mathrm{IL}} * IJL \quad (2)$$

$$J_{\mathrm{RJL}} = w_{\mathrm{RL}} * RJL \quad (3)$$

where w_{IL} and w_{RL} are the weighting factors for the intact and residual knee, respectively, and IJL and RJL are the joint contact forces in units of newtons per body weight for the intact and residual limb, respectively. Separate optimizations were performed to reduce the knee joint contact forces of only the intact limb (IJL), only the residual limb (RJL), and for both limbs (IRJL). When improving sagittal-plane dynamic balance symmetry over the gait cycle (DynBal), the sum of the squared differences between the simulated and experimental whole-body angular momentum about the center of mass normalized by the respective experimental standard deviation squared (Eq. (4)) was added to Eq. (1)

$$J_{\mathrm{WBAM}} = w_{\mathrm{wbam}} * \sum_{i=1}^{n} \frac{\left(Y_i - \hat{Y}_i\right)^2}{\mathrm{SD}_i^2} \quad (4)$$

where w_{wbam} is the weighting factor for the whole-body angular momentum.

Analyses. To assess how closely the simulations emulated the experimental data, the root-mean-square errors were calculated between the simulation and experimental kinematic and GRF data. In addition, the metabolic cost, intact and residual limb knee joint loads, differences in the range of sagittal-plane whole-body angular momentum between the first and second halves of the gait cycle, and the root-mean-square error between simulated and experimental whole-body angular momentum were compared across all simulations. Finally, the magnitude and timing of the prosthetic ankle

torque profile, as well as the net prosthetic ankle work calculated by integrating the prosthetic ankle power profile, were compared across all simulations.

Results

The resulting kinematics and GRFs from all simulations emulated the experimental data within two standard deviations of the mean over the gait cycle (Figs. 2 and 3). For the PASS condition, the average root-mean-square error between the simulated and experimental kinematics and GRFs were 4.2 deg and 0.05 N/BW (2 SDs = 15.7 deg and 0.09 N/BW), respectively (Fig. 2). Across all powered conditions, the average root-mean-square error between the simulated and experimental kinematics and GRFs were 3.5 deg and 0.06 N/BW (2 SDs = 13.9 deg and 0.13 N/BW), respectively (Fig. 3).

Metabolic Cost. All powered conditions had a lower metabolic cost than the PASS condition (Fig. 4) with the POW condition having a 26.5% reduction. Compared to the POW condition, the MC condition had the largest reduction of 7.8%, followed by RJL and the IJL conditions with reductions of 3.1% and 0.3%, respectively. However, the IRJL and DynBal conditions required a higher metabolic cost than the POW condition with increases of 0.7% and 5.9%, respectively.

Knee Joint Loading. All powered conditions decreased the peak knee joint contact force on both the intact limb and residual limb compared to the PASS condition (Fig. 5). The IJL condition had the largest reductions in peak intact limb knee joint force by 4.8 N/BW. In addition, the RJL condition had the largest reduction in peak residual limb joint force by 1.5 N/BW. The IRJL condition demonstrated secondary reductions in both intact limb and residual limb knee joint loads by 4.6 N/BW and 1.4 N/BW, respectively. Interestingly, the IRJL condition improved joint force symmetry the most by having the lowest difference in peak joint force between limbs of 0.4 N/BW. The IJL and MC conditions also improved joint load symmetry compared to the PASS condition with differences of 0.5 and 0.6 N/BW between limbs, respectively.

Dynamic Balance Symmetry. All powered conditions except for the RJL condition improved sagittal-plane dynamic balance symmetry compared to the PASS condition (Table 2). The DynBal condition had the most improved symmetry with the smallest difference in the ranges between the first and second half of the gait cycle of 0.008 (unitless). In addition, the DynBal condition had most improved accuracy between the simulated and experimental whole-body angular momentum profiles with a root mean squared error of 0.005 (unitless).

Prosthetic Ankle-Torque and Work. Compared to the PASS condition, the powered conditions exhibited an overall increase in peak plantarflexor torque during mid- to late stance (Fig. 6(*a*)). The average increase in peak plantarflexor torque from the PASS condition was 14.9 N·m with the largest increase from the IRJL condition having a difference of 16.7 N·m. The timing of the peak plantarflexor torque was similar for all conditions. The plantarflexor torque timing varied the most during the first 40% of the gait cycle and resulted in differences in net prosthetic ankle work, especially among the powered conditions.

All powered conditions had positive net prosthetic work compared to the negative net prosthetic work in the PASS condition (Fig. 6(*b*)). Compared to the POW condition, the IJL, DynBal, and MC conditions produced lower net work by 1.1, 2.0, and 3.5 J, respectively. However, the RJL and IRJL conditions had greater

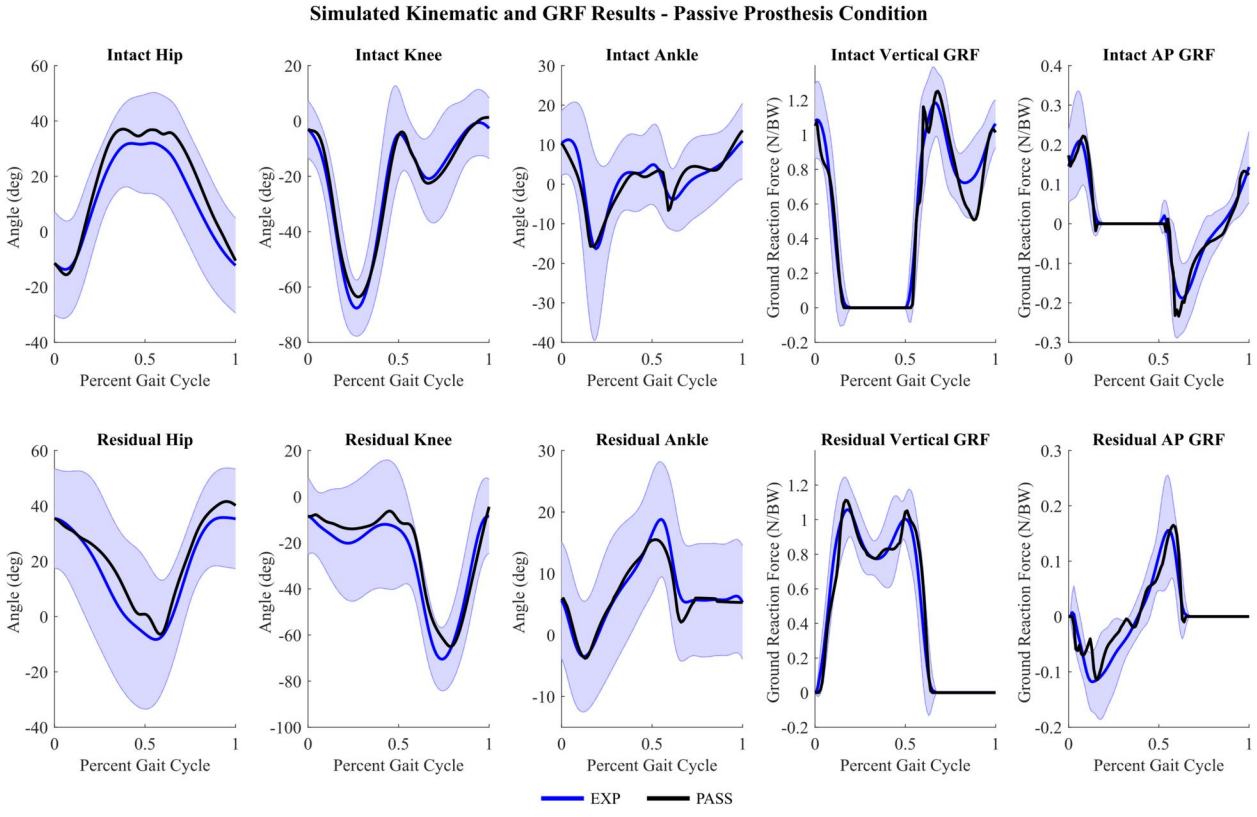

Fig. 2 Simulated kinematics and GRF profiles for the passive prosthesis condition (PASS) that tracked the experimental walking pattern of individuals with TTA (EXP). Shaded areas represent ±2 SD from the experimental mean.

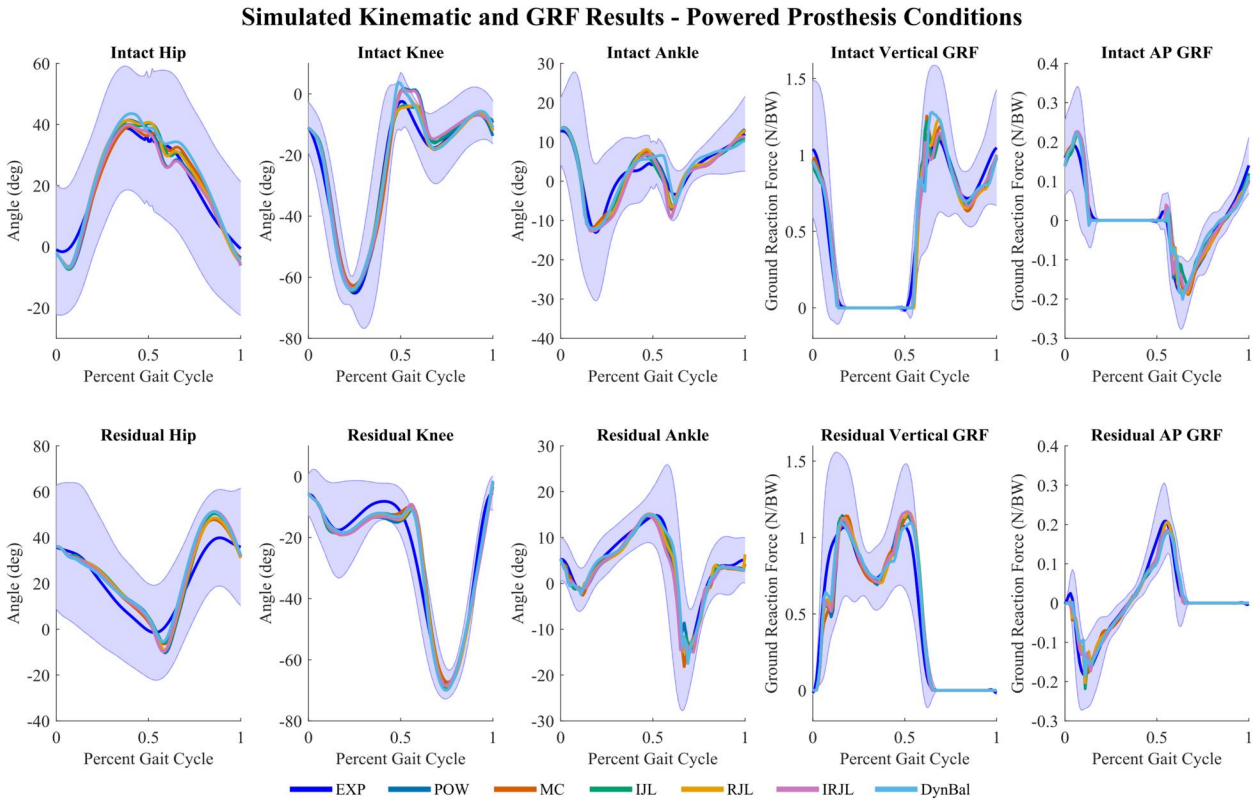

Fig. 3 Simulated kinematics and GRF profiles for each powered prosthesis condition (POW, MC, IJL, RJL, IRJL, and DynBal) that tracked the walking pattern of able-bodied individuals (EXP). Shaded areas represent ±2 SD from the experimental mean.

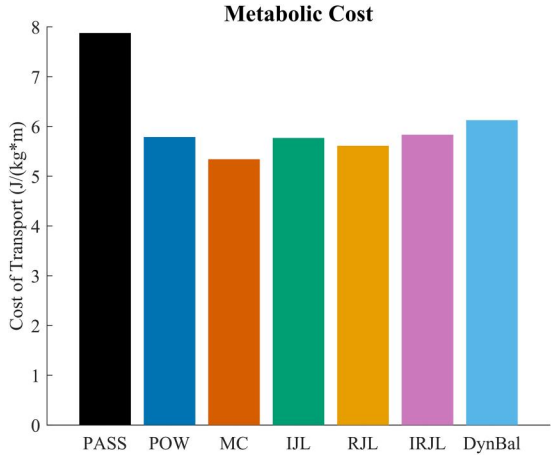

Fig. 4 Total metabolic cost for each simulated condition.

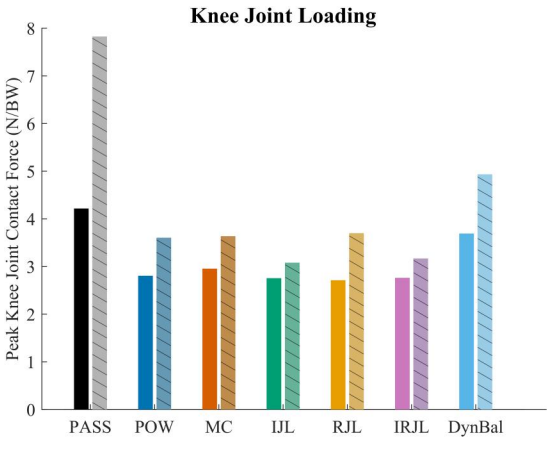

Fig. 5 Peak knee joint contact force for the residual (solid) and intact (striped) limbs for each simulated condition.

Table 2 Peak-to-peak ranges of whole-body angular momentum during the first and second halves of the gait cycle for all conditions

Whole-body angular momentum results							
	PASS	POW	MC	IJL	RJL	IRJL	DynBal
First half range	0.068	0.041	0.041	0.039	0.041	0.040	0.040
Second half range	0.042	0.022	0.029	0.028	0.027	0.020	0.032
Difference	0.026	0.019	0.012	0.011	0.014	0.020	0.008
RMSE	0.014	0.007	0.006	0.007	0.007	0.008	0.005

Differences in ranges are presented to quantify symmetry, while root-mean-square error (RMSE) quantifies how well the simulation reproduced able-bodied whole-body angular momentum.

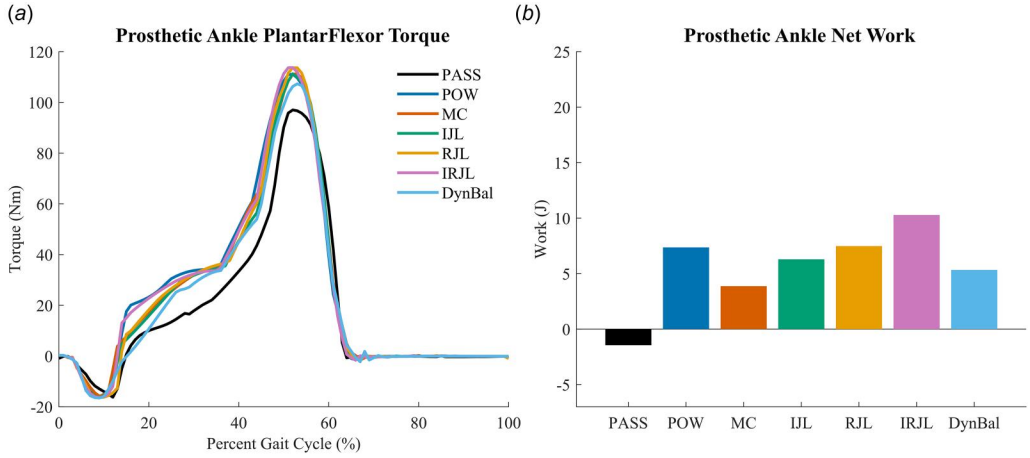

Fig. 6 (*a*) Simulated prosthetic torque profiles and (*b*) net prosthetic work from the optimal torque profiles of the passive and powered conditions.

positive net work than the POW condition by 0.1 and 2.9 J, respectively.

Discussion

The purpose of this study was to optimize the ankle torque profile of a powered prosthesis to improve metabolic cost, knee joint loading, and sagittal-plane dynamic balance during walking using a musculoskeletal simulation-based optimization framework. We expected to see distinct torque profiles that improved each measure of walking performance, which was supported with interesting tradeoffs for each measure.

Metabolic Cost. Metabolic cost was reduced from the PASS to powered conditions with the greatest reductions by the MC condition. The relative differences in metabolic cost between a passive versus a powered prosthesis under these conditions (∼26.5%) were greater than reported differences in previous experimental studies between a passive and powered ankle prosthesis (7–20%) [29,30] as well as able-bodied controls (15–16%) [2,3]. In addition, previous studies have also shown that metabolic cost decreases with an increase in positive ankle-prosthetic work [29–31], which we also observed between the PASS and POW conditions. However, we found that this trend did not continue as the MC condition reduced the metabolic cost the most from the PASS condition with a net prosthetic work that was less than the POW condition. A previous modeling study also found a nonlinear relationship between prosthetic work and metabolic cost [14], which suggests that factors other than increased positive prosthetic work can lead to reductions in metabolic cost.

To explain how the MC condition had the least metabolic cost, we performed a post-hoc analysis of the individual muscle group contributions to the total metabolic cost over the stance and swing phases of the gait cycle (Fig. 7). The MC condition showed the greatest metabolic cost reductions in the residual limb gluteus maximus, residual limb rectus femoris, and intact limb iliopsoas during stance; the residual limb hamstrings and vasti during swing; and the bicep femoris short head and gluteus medius during both phases (Fig. 7). The PASS condition had a higher metabolic cost for these muscle groups, which is consistent with previous studies that have observed similar trends as a compensatory mechanism that individuals with TTA commonly use during walking [32,33]. These findings suggest that the optimal ankle torque profile, as seen in the MC condition, must be appropriately tuned to reduce proximal muscle use during the gait cycle for effective metabolic cost reductions.

Knee Joint Loading. The PASS condition produced the highest intact limb load of over 7 N/BW, which is higher than the joint contact load of 4.5 N/BW from previous simulation work [34] and the 2.3–2.6 N/BW from in vivo knee implant studies [35–37]. However, when using a powered foot and incorporating measures of demand in the optimization cost function (i.e., POW, MC, and IRJL conditions), the joint loads of both limbs (2.7–4.9 N/BW) are closer to the previous in vivo (2.3–2.6 N/BW) and computational (2.5–4.5 N/BW) [38,39] estimates of able-bodied knee joint contact loads. These results suggest that the central nervous system may use measures of demand to help coordinate muscle activity during walking.

All powered conditions had a torque profile that produced net positive work that effectively decreased knee joint loads of both limbs relative to the PASS condition, which is consistent with previous studies finding an association between positive mechanical work and decreased intact limb knee joint loads [4,10]. This result suggests that the net positive work output from a powered prosthesis may reduce the risk of secondary injuries that develop from high repetitive loads. However, further increases in prosthetic work across powered conditions did not result in further reductions in intact limb or residual limb knee joint loading, which suggests that greater net prosthetic work from a powered prosthesis does not necessarily improve knee joint loading.

To gain further insight into the relationship between prosthetic work and knee joint loading, we performed a post-hoc analysis (Fig. 8) comparing individual musculotendon work across conditions during early stance of each limb where the peak knee joint load occurred (Fig. 9). The IJL condition had decreased magnitude of intact limb vasti muscle work, but also had increased positive intact limb gluteus maximus work, which a previous study also observed when analyzing a quadricep avoidance gait [40]. The RJL condition had the most reduced residual limb hamstring work, suggesting that the powered ankle push-off work was optimally tuned to reduce knee flexor muscle activity, which would then reduce knee joint loads. Finally, the IRJL condition demonstrated the combined musculotendon work trends of the IJL and RJL conditions but not to the same degree, which resulted in the lesser reductions in knee joint loads for both limbs. These findings suggest that reducing knee joint loads effectively using an optimal powered prosthesis torque profile requires the precise timing of appropriate prosthetic work to offload muscles that cross the knee.

Interestingly, knee joint load symmetry improved between the PASS and POW conditions and further between the MC, IJL, and IRJL conditions and the PASS condition. A previous study demonstrated that improved knee moment symmetry reduces intact limb knee loading [41], but they did not analyze the effects of knee

moment symmetry on other measures of walking performance, such as metabolic cost or whole-body angular momentum. Thus, future work seeking to optimize the prosthesis torque profile should focus on knee joint symmetry for improved walking mechanics.

Dynamic Balance Symmetry. The torque profile in the DynBal condition best produced whole-body angular momentum that was the most symmetrical between the first and second halves of the gait cycle and the most similar to that of the able-bodied experimental data. Since the powered conditions specifically enforced near symmetrical kinematics and GRFs by tracking the walking patterns of able-bodied individuals, the powered prosthesis of these conditions produced a torque profile similar to the combination of the GAS and SOL muscles, which provide needed backwards rotation in the latter half of the gait cycle to produce symmetrical whole-body angular momentum [42]. Furthermore, the additional measure in the cost function from the DynBal condition altered the timing and peak magnitude of the torque profile (Fig. 6), coordinating the lower-limb muscle activity and the torque profile to better reproduce able-bodied whole-body angular momentum.

Muscle Trends Between Passive and Powered Conditions. The post-hoc analyses not only helped explain the study results but also revealed muscle trends that the powered conditions shared when compared to the passive condition. The powered conditions showed decreased residual limb hamstring and comparable or greater residual limb gluteus maximus metabolic cost during residual limb stance phase metabolic cost (Fig. 7) and musculotendon work during early stance of the residual limb (Fig. 8). These muscles have been previously found to provide body propulsion and support, respectively [43], which suggests that the additional power from the powered prostheses shifts the hip extensor demand from the residual limb hamstring to the residual limb gluteus maximus to provide more body support than propulsion during stance. In addition, the powered conditions had decreased metabolic cost in the residual limb bicep femoris short head, iliopsoas, and vasti during residual limb swing phase compared to the passive condition (Fig. 7), which suggests that the powered prostheses helped initiate leg swing normally provided by the gastrocnemius [44] and reduce the compensatory muscles necessary to perform this function when using a passive prosthesis. Furthermore, the powered conditions showed decreased negative intact limb rectus femoris work and positive intact limb hamstrings work relative to the passive condition during the early intact limb stance (Fig. 8). Since individuals with TTA use their intact limb hamstrings to compensate for the lack of plantarflexor propulsion [32,33], the intact limb rectus femoris eccentric work increases to control knee flexion, and both were reduced when using the powered prosthesis. Overall, the additional power from a powered prosthesis redistributed muscle work to reduce the overall muscle demand associated with needed compensatory mechanisms when using a passive prosthesis.

Tradeoffs in Walking Performance. While each of the conditions focused on improving one aspect of walking performance for individuals with TTA, we found that other measures of walking performance were also affected. For example, we found the torque profile of the DynBal condition adversely affected metabolic cost, knee joint loading, and knee joint load symmetry between limbs compared to other powered conditions. Pareto-front relationships between measures have also been observed in other optimal control simulation studies [41,45]. Alternatively, some of our other results suggest that an improvement in one aspect of walking performance also causes improvements in other measures, such as the improvement of knee joint loading also improved the metabolic cost in both the IJL and RJL conditions compared to the POW condition. These findings suggest the torque profile of powered prostheses can be optimally tuned to improve multiple measures of walking performance depending on the goals of the user.

Limitations and Future Work. This study was performed with several assumptions that should be considered when interpreting the results. First, we used a 2D musculoskeletal model with a limited number of muscle groups and a prosthesis with no socket movement, which was similar to previous studies to run computationally feasible optimizations [41,46]. While simpler models would affect the accuracy of sensitive measures, such as metabolic cost, the relative differences between conditions were consistent with previous studies. Further, the model used an ideal external actuator at the ankle to generate the torque profiles. However, the peak torque (∼104–127 N·m) and the maximum net work (IRJL: ∼19 J) from this study were within range of current commercial and research prosthesis peak torque capabilities (120–140 N·m) [47–50] and are consistent with the outputs in other experimental walking studies (peak torque: ∼120–130 N·m; net work: ∼0.13–0.17 J/kg) [10,29,51]. We also tracked group averaged kinematics and GRFs, which limits the generalizability of the results. Future research should apply this computational framework to optimize prosthetic ankle torque for subject-specific walking mechanics to see how the torque profiles vary across individuals. Another potential limitation is that muscle contributions to knee joint loading could not be calculated as a post-hoc analysis as SCONE does not support this feature. This led us to use musculotendon work as a surrogate to explain our results, and these results were consistent with previous studies. Finally, we used a stochastic optimizer to solve a multi-objective optimization problem with a high-dimensional search space, which may not guarantee a global minimum. However, we initiated multiple simulations at different random seeds and updated the initial parameters after each simulation with the best tracking results to help improve convergence toward a near-global solution.

Conclusion

This study aimed to identify the torque profiles of a powered prosthesis that improve metabolic cost, knee joint loading, and sagittal-plane dynamic balance during steady-state walking in individuals with transtibial amputations. We found there were unique optimal prosthetic torque profiles that improved the various measures of walking performance, where prosthetic torque timing throughout the gait cycle was found to be critical to these improvements. Furthermore, tradeoffs between measures were observed, highlighting the need for optimizations to analyze multiple biomechanical measures within a single cost function. Overall, this work provides a framework for future work developing more elaborate and customized controllers for powered prostheses to improve other biomechanical measures in individuals with TTA gait.

Acknowledgment

The authors would like to thank Stephanie Molitor, Ph.D., for providing the processed dataset and valuable comments on the paper, as well as Kristen Stewart, M.S., Shelby Walford, Ph.D., and Helen Emerson, B.S., for their constructive feedback.

Funding Data

- U.S. Department of Veterans Affairs Rehabilitation Research, Development, and Translation (RX003138 and RX002974).

Data Availability Statement

The datasets generated and supporting the findings of this article are obtainable from the corresponding author upon reasonable request.

Appendix

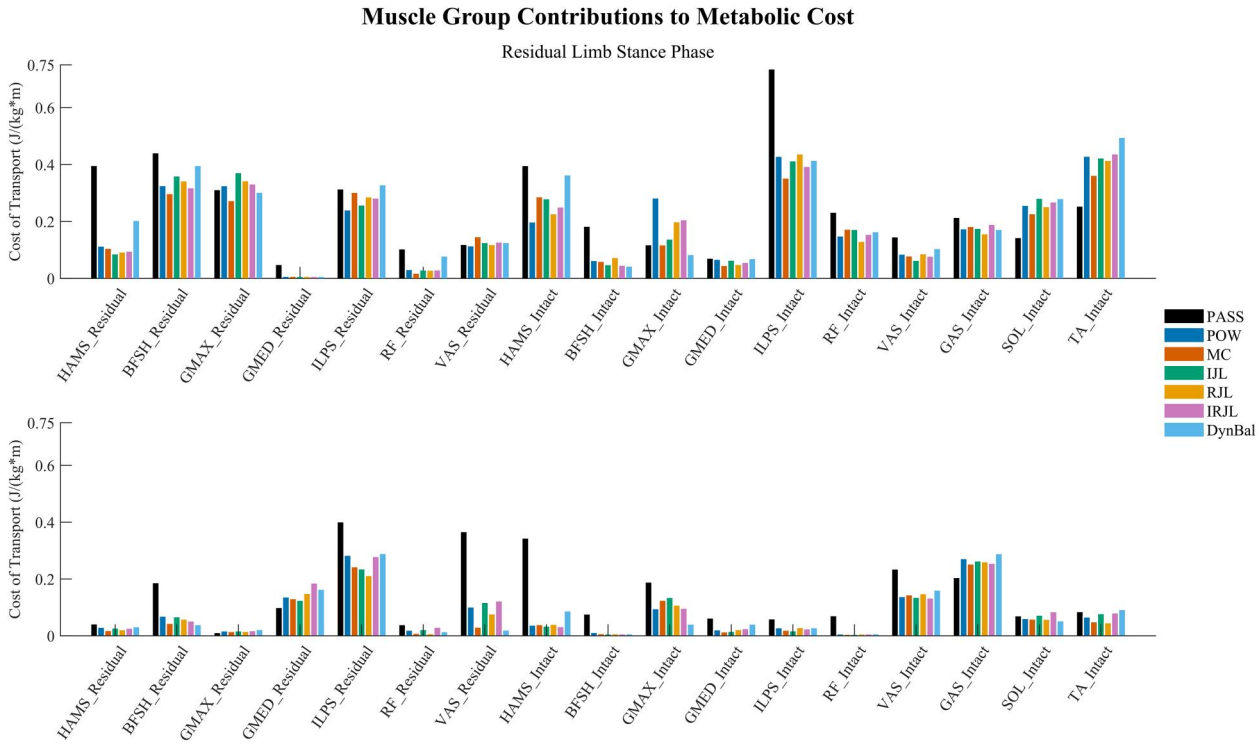

Fig. 7 Individual muscle group contributions to the total metabolic cost during the residual limb stance and swing phases of the gait cycle for each condition.

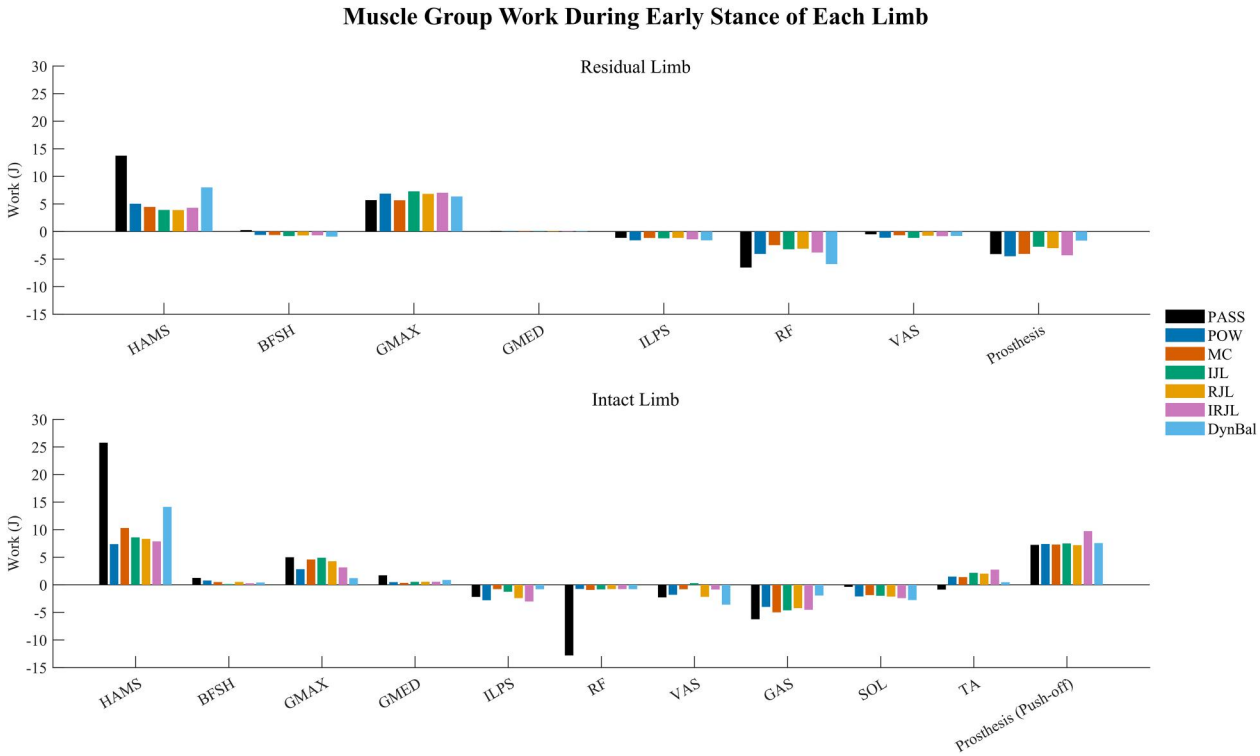

Fig. 8 Individual musculotendon group and prosthetic work during the early stance phase of each limb for each condition. Prosthesis (push-off) work in the intact limb represents the push-off work done during double support.

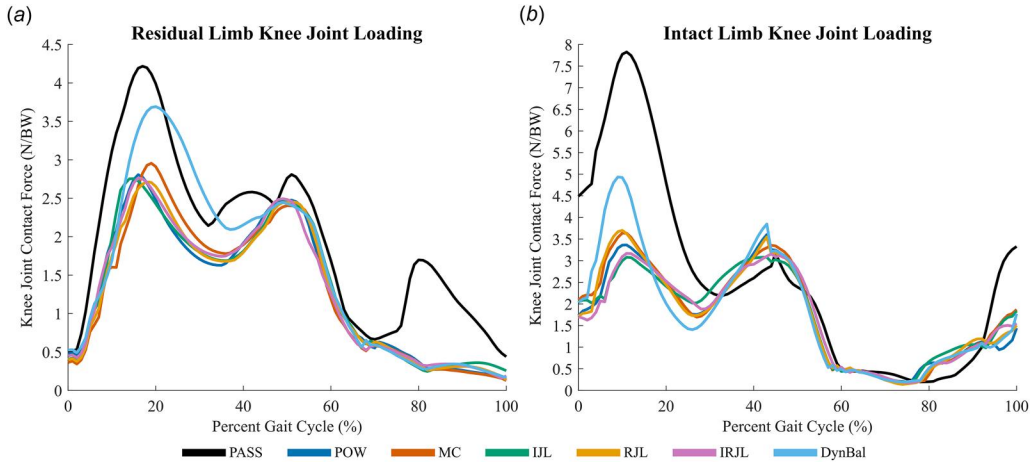

Fig. 9 The (*a*) residual and (*b*) intact limb knee joint loading for each condition over a single stride from heel strike to heel strike of each respective limb. Note, the vertical scales are different between the limbs.

References

[1] Gailey, R., 2008, "Review of Secondary Physical Conditions Associated With Lower-Limb Amputation and Long-Term Prosthesis Use," J. Rehabil. Res. Dev., **45**(1), pp. 15–30.

[2] Gailey, R. S., Wenger, M. A., Raya, M., Kirk, N., Erbs, K., Spyropoulos, P., and Nash, M. S., 1994, "Energy Expenditure of Trans-Tibial Amputees During Ambulation at Self-Selected Pace," Prosthet. Orthot. Int., **18**(2), pp. 84–91.

[3] Genin, J. J., Bastien, G. J., Franck, B., Detrembleur, C., and Willems, P. A., 2008, "Effect of Speed on the Energy Cost of Walking in Unilateral Traumatic Lower Limb Amputees," Eur. J. Appl. Physiol., **103**(6), pp. 655–663.

[4] Morgenroth, D. C., Segal, A. D., Zelik, K. E., Czerniecki, J. M., Klute, G. K., Adamczyk, P. G., Orendurff, M. S., Hahn, M. E., Collins, S. H., and Kuo, A. D., 2011, "The Effect of Prosthetic Foot Push-Off on Mechanical Loading Associated With Knee Osteoarthritis in Lower Extremity Amputees," Gait Posture, **34**(4), pp. 502–507.

[5] Mak, A. F. T., Zhang, M., and Boone, D. A., 2001, "State-of-the-Art Research in Lower-Limb Prosthetic Biomechanics-Socket Interface: A Review," J. Rehabil. Res. Dev., **38**(2), pp. 161–174.

[6] Miller, W. C., Speechley, M., and Deathe, B., 2001, "The Prevalence and Risk Factors of Falling and Fear of Falling Among Lower Extremity Amputees," Arch. Phys. Med. Rehabil., **82**(8), pp. 1031–1037.

[7] Silverman, A. K., and Neptune, R. R., 2011, "Differences in Whole-Body Angular Momentum Between Below-Knee Amputees and Non-Amputees Across Walking Speeds," J. Biomech., **44**(3), pp. 379–385.

[8] Russell Esposito, E., Aldridge Whitehead, J. M., and Wilken, J. M., 2016, "Step-to-Step Transition Work During Level and Inclined Walking Using Passive and Powered Ankle–Foot Prostheses," Prosthet. Orthot. Int., **40**(3), pp. 311–319.

[9] Herr, H. M., and Grabowski, A. M., 2012, "Bionic Ankle–Foot Prosthesis Normalizes Walking Gait for Persons With Leg Amputation," Proc. R. Soc. B Biol. Sci., **279**(1728), pp. 457–464.

[10] Grabowski, A. M., and D'Andrea, S., 2013, "Effects of a Powered Ankle-Foot Prosthesis on Kinetic Loading of the Unaffected Leg During Level-Ground Walking," J. NeuroEng. Rehabil., **10**(1), p. 49.

[11] D'Andrea, S., Wilhelm, N., Silverman, A. K., and Grabowski, A. M., 2014, "Does Use of a Powered Ankle-Foot Prosthesis Restore Whole-Body Angular Momentum During Walking at Different Speeds?," Clin. Orthop. Relat. Res., **472**(10), pp. 3044–3054.

[12] Ackermann, M., and van den Bogert, A. J., 2010, "Optimality Principles for Model-Based Prediction of Human Gait," J. Biomech., **43**(6), pp. 1055–1060.

[13] Falisse, A., Serrancolí, G., Dembia, C. L., Gillis, J., Jonkers, I., and De Groote, F., 2019, "Rapid Predictive Simulations With Complex Musculoskeletal Models Suggest That Diverse Healthy and Pathological Human Gaits Can Emerge From Similar Control Strategies," J. R. Soc. Interface, **16**(157), p. 20190402.

[14] Handford, M. L., and Srinivasan, M., 2018, "Energy-Optimal Human Walking With Feedback-Controlled Robotic Prostheses: A Computational Study," IEEE Trans. Neural Syst. Rehabil. Eng., **26**(9), pp. 1773–1782.

[15] Ardianuari, S., Cyr, K. M., Neptune, R. R., and Klute, G. K., 2024, "Should Individuals With Unilateral Transtibial Amputation Carry a Load on Their Intact or Prosthetic Side?," J. Biomech., **177**, p. 112385.

[16] Molina, L. K., Small, G. H., and Neptune, R. R., 2023, "The Influence of Step Width on Balance Control and Response Strategies During Perturbed Walking in Healthy Young Adults," J. Biomech., **157**, p. 111731.

[17] Ong, C. F., Geijtenbeek, T., Hicks, J. L., and Delp, S. L., 2019, "Predicting Gait Adaptations Due to Ankle Plantarflexor Muscle Weakness and Contracture Using Physics-Based Musculoskeletal Simulations," PLoS Comput. Biol., **15**(10), p. e1006993.

[18] Yamaguchi, G. T., 2001, *Dynamic Modeling of Musculoskeletal Motion*, Springer US, Boston.

[19] Sherman, M. A., Seth, A., and Delp, S. L., 2011, "Simbody: Multibody Dynamics for Biomedical Research," Procedia IUTAM, **2**, pp. 241–261.

[20] Ding, Y., Kim, M., Kuindersma, S., and Walsh, C. J., 2018, "Human-in-the-Loop Optimization of Hip Assistance With a Soft Exosuit During Walking," Sci. Rob., **3**(15), p. eaar5438.

[21] Perry, J., and Burnfield, J. M., 2010, *Gait Analysis: Normal and Pathological Function*, 2nd ed., SLACK Incorporated, Thorofare, NJ.

[22] Geyer, H., and Herr, H., 2010, "A Muscle-Reflex Model That Encodes Principles of Legged Mechanics Produces Human Walking Dynamics and Muscle Activities," IEEE Trans. Neural Syst. Rehabil. Eng., **18**(3), pp. 263–273.

[23] LaPrè, A. K., Price, M. A., Wedge, R. D., Umberger, B. R., and Sup, F. C., IV, 2018, "Approach for Gait Analysis in Persons With Limb Loss Including Residuum and Prosthesis Socket Dynamics," Int. J. Numer. Methods Biomed. Eng., **34**(4), p. e2936.

[24] Geijtenbeek, T., 2019, "SCONE: Open Source Software for Predictive Simulation of Biological Motion," J. Open Source Software, **4**(38), p. 1421.

[25] Hansen, N., 2006, "The CMA Evolution Strategy: A Comparing Review," *Towards a New Evolutionary Computation: Advances in the Estimation of Distribution Algorithms*, J. A. Lozano, P. Larrañaga, I. Inza, and E. Bengoetxea, eds., Springer Berlin Heidelberg, Berlin, Heidelberg, Germany, pp. 75–102.

[26] Van Den Bogert, A. J., Blana, D., and Heinrich, D., 2011, "Implicit Methods for Efficient Musculoskeletal Simulation and Optimal Control," Procedia IUTAM, **2**, pp. 297–316.

[27] Bhargava, L. J., Pandy, M. G., and Anderson, F. C., 2004, "A Phenomenological Model for Estimating Metabolic Energy Consumption in Muscle Contraction," J. Biomech., **37**(1), pp. 81–88.

[28] Wang, J. M., Hamner, S. R., Delp, S. L., and Koltun, V., 2012, "Optimizing Locomotion Controllers Using Biologically-Based Actuators and Objectives," ACM Trans. Graphics, **31**(4), pp. 1–11.

[29] Au, S. K., Weber, J., and Herr, H., 2009, "Powered Ankle–Foot Prosthesis Improves Walking Metabolic Economy," IEEE Trans. Rob., **25**(1), pp. 51–66.

[30] Caputo, J. M., and Collins, S. H., 2014, "Prosthetic Ankle Push-Off Work Reduces Metabolic Rate but Not Collision Work in Non-Amputee Walking," Sci. Rep., **4**(1), p. 7213.

[31] Ingraham, K. A., Choi, H., Gardinier, E. S., Remy, C. D., and Gates, D. H., 2018, "Choosing Appropriate Prosthetic Ankle Work to Reduce the Metabolic Cost of Individuals With Transtibial Amputation," Sci. Rep., **8**(1), p. 15303.

[32] Nolan, L., and Lees, A., 2000, "The Functional Demands on the Intact Limb During Walking for Active Transfemoral and Transtibial Amputees," Prosthet. Orthot. Int., **24**(2), pp. 117–125.

[33] Winter, D. A., and Sienko, S. E., 1988, "Biomechanics of Below-Knee Amputee Gait," J. Biomech., **21**(5), pp. 361–367.

[34] Silverman, A. K., and Neptune, R. R., 2014, "Three-Dimensional Knee Joint Contact Forces During Walking in Unilateral Transtibial Amputees," J. Biomech., **47**(11), pp. 2556–2562.

[35] D'Lima, D. D., Patil, S., Steklov, N., Chien, S., and Colwell, C. W., 2007, "In vivo Knee Moments and Shear After Total Knee Arthroplasty," J. Biomech., **40**, pp. S11–S17.

[36] Kutzner, I., Heinlein, B., Graichen, F., Bender, A., Rohlmann, A., Halder, A., Beier, A., and Bergmann, G., 2010, "Loading of the Knee Joint During Activities of Daily Living Measured In vivo in Five Subjects," J. Biomech., **43**(11), pp. 2164–2173.

[37] Mündermann, A., Dyrby, C. O., D'Lima, D. D., Colwell, C. W., Jr., and Andriacchi, T. P., 2008, "In vivo Knee Loading Characteristics During Activities

of Daily Living as Measured by an Instrumented Total Knee Replacement," J. Orthop. Res., **26**(9), pp. 1167–1172.
[38] Kumar, D., Manal, K. T., and Rudolph, K. S., 2013, "Knee Joint Loading During Gait in Healthy Controls and Individuals With Knee Osteoarthritis," Osteoarthritis Cartil. OARS Osteoarthritis Res. Soc., **21**(2), pp. 298–305.
[39] Winby, C. R., Lloyd, D. G., Besier, T. F., and Kirk, T. B., 2009, "Muscle and External Load Contribution to Knee Joint Contact Loads During Normal Gait," J. Biomech., **42**(14), pp. 2294–2300.
[40] Sasaki, K., and Neptune, R. R., 2010, "Individual Muscle Contributions to the Axial Knee Joint Contact Force During Normal Walking," J. Biomech., **43**(14), pp. 2780–2784.
[41] Koelewijn, A. D., and van den Bogert, A. J., 2016, "Joint Contact Forces Can Be Reduced by Improving Joint Moment Symmetry in Below-Knee Amputee Gait Simulations," Gait Posture, **49**, pp. 219–225.
[42] Neptune, R. R., and McGowan, C. P., 2011, "Muscle Contributions to Whole-Body Sagittal Plane Angular Momentum During Walking," J. Biomech., **44**(1), pp. 6–12.
[43] Silverman, A. K., and Neptune, R. R., 2012, "Muscle and Prosthesis Contributions to Amputee Walking Mechanics: A Modeling Study," J. Biomech., **45**(13), pp. 2271–2278.
[44] Neptune, R. R., Kautz, S. A., and Zajac, F. E., 2001, "Contributions of the Individual Ankle Plantar Flexors to Support, Forward Progression and Swing Initiation During Walking," J. Biomech., **34**(11), pp. 1387–1398.
[45] Koelewijn, A. D., Dorschky, E., and van den Bogert, A. J., 2018, "A Metabolic Energy Expenditure Model With a Continuous First Derivative and Its Application to Predictive Simulations of Gait," Comput. Methods Biomech. Biomed. Eng., **21**(8), pp. 521–531.
[46] Handford, M. L., and Srinivasan, M., 2016, "Robotic Lower Limb Prosthesis Design Through Simultaneous Computer Optimizations of Human and Prosthesis Costs," Sci. Rep., **6**(1), p. 19983.
[47] Au, S., and Herr, H., 2008, "Powered Ankle-Foot Prosthesis," IEEE Rob. Autom. Mag., **15**(3), pp. 52–59.
[48] Azocar, A. F., Mooney, L. M., Duval, J.-F., Simon, A. M., Hargrove, L. J., and Rouse, E. J., 2020, "Design and Clinical Implementation of an Open-Source Bionic Leg," Nat. Biomed. Eng., **4**(10), pp. 941–953.
[49] Gabert, L., Hood, S., Tran, M., Cempini, M., and Lenzi, T., 2020, "A Compact, Lightweight Robotic Ankle-Foot Prosthesis: Featuring a Powered Polycentric Design," IEEE Rob. Autom. Mag., **27**(1), pp. 87–102.
[50] Grimmer, M., Holgate, M., Holgate, R., Boehler, A., Ward, J., Hollander, K., Sugar, T., and Seyfarth, A., 2016, "A Powered Prosthetic Ankle Joint for Walking and Running," Biomed. Eng. OnLine, **15**(S3), p. 141.
[51] Ferris, A. E., Aldridge, J. M., Rábago, C. A., and Wilken, J. M., 2012, "Evaluation of a Powered Ankle-Foot Prosthetic System During Walking," Arch. Phys. Med. Rehabil., **93**(11), pp. 1911–1918.